



Article

Assessing the Discriminatory Capabilities of iEK Devices under DC and DC-Biased AC Stimulation Potentials

Nuzhet Nihaar Nasir Ahamed ¹, Carlos A. Mendiola-Escobedo ², Victor H. Perez-Gonzalez ^{2,*} and Blanca H. Lapizco-Encinas ^{1,*}

- ¹ Microscale Bioseparations Laboratory and Biomedical Engineering Department, Rochester Institute of Technology, 160 Lomb Memorial Drive, Rochester, NY 14623, USA; nn5878@rit.edu
- ² School of Engineering and Sciences, Tecnologico de Monterrey, Monterrey 64849, Mexico; carlos_mendiola2000@hotmail.com
- * Correspondence: vhpg@tec.mx (V.H.P.-G.); bhlbme@rit.edu (B.H.L.-E.)

Abstract: There is a rising need for rapid and reliable analytical methods for separating microorganisms in clinical and biomedical applications. Microscale-insulator-based electrokinetic (iEK) systems have proven to be robust platforms for assessing a wide variety of microorganisms. Traditionally, iEK systems are usually stimulated with direct-current (DC) potentials. This work presents a comparison between using DC potentials and using DC-biased alternating-current (AC) potentials in iEK systems for the separation of microorganisms. The present study, which includes mathematical modeling and experimentation, compares the separation of bacterial and yeast cells in two distinct modes by using DC and DC-biased AC potentials. The quality of both separations, assessed in terms of separation resolution (R_s), showed a complete separation (R_s = 1.51) with the application of a DC-biased low-frequency AC signal but an incomplete separation (R_s = 0.55) with the application of an RMS-equivalent DC signal. Good reproducibility between experimental repetitions (<10%) was obtained, and good agreement (~18% deviation) was observed between modeling and experimental retention times. The present study demonstrates the potential of extending the limits of iEK systems by employing DC-biased AC potentials to perform discriminatory separations of microorganisms that are difficult to separate with the application of DC potentials.

Keywords: electrokinetics; electroosmosis; electrophoresis; separation; electropherogram

Citation: Nasir Ahamed, N.N.;
Mendiola-Escobedo, C.A.;
Perez-Gonzalez, V.H.;
Lapizco-Encinas, B.H. Assessing the
Discriminatory Capabilities of iEK
Devices under DC and DC-Biased
AC Stimulation Potentials.
Micromachines 2023, 14, x.
https://doi.org/10.3390/xxxxx

Academic Editor: Antonio Ramos

Received: 18 November 2023 Revised: 9 December 2023 Accepted: 11 December 2023 Published: date



Copyright: © 2023 by the authors. Submitted for possible open access publication under the terms and conditions of the Creative Commons Attribution (CC BY) license (https://creativecommons.org/licenses/by/4.0/).

1. Introduction

There is a growing need for rapid and reliable methods for the analytical separation of microorganisms in clinical analysis, food safety, and environmental monitoring assessments [1]. There is a plethora of well-established traditional separation techniques for the separation of nanosized analytes (e.g., macromolecules), such as capillary electrophoresis (CE) and liquid chromatography (LC), which are customizable to different target analytes [2,3]. However, there is a lack of well-developed and customizable methods for separating micron-sized analytes, such as microorganisms [1]. Microscale electrokinetic (EK) methods offer an attractive option for analyzing and separating microorganisms due to their attractive characteristics, such as low sample requirements, low cost, high resolution, robustness, and ease of optimization [4,5]. Insulator-based EK (iEK) microfluidic devices have proven to be efficient platforms for assessing a wide range of microorganisms, ranging from viruses to mammalian cells [6]. The presence of three-dimensional (3D) insulating posts or structures within a microchannel distorts the electric field distribution in the iEK device, forming zones of higher electric field intensity and giving rise to nonlinear EK phenomena [7]. Therefore, these systems have the added advantage of combining linear and nonlinear EK effects within the same system, which can be strategically manipulated for separating complex mixtures [7].

The assessment and separation of intact microorganisms with CE systems have been investigated by several research groups, including the Armstrong [8–12], Horká [13–17], and Buszewski [18–22] groups. Intact microbes have also been analyzed with microfluidic iEK systems; for example, the Hayes group reported high-resolution separations of closely related microbial strains [23–25]. Our group reported the separation of viruses, bacterial cells, and yeast cells [7]. However, all these separations utilized direct-current (DC) voltages. There are only a few studies that report the separation of microorganisms by applying alternating-current (AC) voltages [26–29], such as studies by the Ros group [26–28], the Xuan group [30,31], and our group [29]. The Morgan group [32,33] has also developed iEK systems stimulated with low-frequency AC potentials, but they separated microparticles only, not microorganisms. However, despite the availability of reports illustrating the separation of microorganisms with the two types of stimulation (i.e., DC-only vs. DC-biased AC potentials), a baseline comparison has not been performed, necessitating further investigation.

Until recently, dielectrophoresis (DEP) was considered to be the major, dominant EK phenomenon in iEK systems stimulated with DC or low-frequency (<1 kHz) AC potentials [34]. Although nonlinear electrophoresis (EP_{NL}) was first reported in the 1970s by Dukhin [35], the lack of experiments on EP_{NL} hampered its application [36]. Therefore, the majority of iEK studies ignored the effects of EP_{NL}, leading to inaccurate interpretations and prompting the use of correction factors in mathematical models to match experimental results [37]. Recent reports have highlighted the significant effects of EP_{NL} on particle electromigration in iEK systems that have been used for differentiating microparticles and cells [38–42]. Our group considered the EP_{NL} effect in recent reports on the separation of microparticles and cells with similar characteristics by applying either DC or low-frequency AC signals [7,43]. However, none of these studies included a comparison between separations carried out with DC potentials and separations carried out with AC potentials.

The present study addresses this knowledge gap by demonstrating the separation of microorganisms by employing two types of signals—a DC signal and a low-frequency DC-biased AC signal, of which the DC signal was designed to be equivalent in magnitude to the root mean square (RMS) of the DC-biased AC voltage. The two separations presented here employed a binary mixture of microorganisms, Escherichia coli (E. coli) and Saccharomyces cerevisiae (S. cerevisiae), which are cells of two distinct domains: prokaryotic and eukaryotic, respectively. To the best of our knowledge, this is the first report comparing the performance of DC-stimulated and DC-biased AC-stimulated iEK separation of microorganisms, where the DC potential is equivalent to the RMS value of the DC-biased AC potential. This work included both numerical modeling with COMSOL Multiphysics version 5.6 and experimentation. The quality of these separations was compared by assessing the electropherograms in terms of separation resolution (R_s) . The experimental results indicated that separation resolution values of $R_s = 0.55$ and $R_s = 1.51$ were obtained by applying the DC and the DC-biased AC potentials, respectively. These findings illustrate the added advantage of using AC voltages, which enable separations that are not possible using DC voltages. AC potentials have extra characteristics (frequency, amplitude, and magnitude of the DC bias) that can be modified or customized to enable a desired separation process. Good reproducibility between experimental repetitions, ranging from 2 to 8%, was obtained. The deviations between mathematically predicted and experimental retention times ranged from 5.5 to 18.2%, indicating that the model is a valuable tool for guidance in the design of separation processes. Joule heating was not considered in this study based on our previous publication [44], where no significant heating occurred. These results demonstrate the ability of AC-stimulated iEK systems to separate microorganisms by offering extra parameters that can be tuned to achieve separations that are not possible employing a DC voltage.

2. Theory

EK phenomena are classified as linear or nonlinear according to their dependence on the electric field. The linear EK phenomena considered here are electroosmosis (EO) and linear electrophoresis (EPL), whose velocities, given by $\mathbf{E} = E\hat{\mathbf{a}}_E$ (where $\hat{\mathbf{a}}_E$ is a unit vector with the direction of vector \mathbf{E} , having a magnitude of E), can be expressed as [43]:

$$\mathbf{v}_{EO} = \mu_{EO} \mathbf{E} = -\frac{\varepsilon_m \zeta_W}{\eta} \mathbf{E} \tag{1}$$

$$\mathbf{v}_{EP,L} = \mu_{EP,L} \mathbf{E} = \frac{\varepsilon_m \zeta_P}{n} \mathbf{E}$$
 (weak field regime) (2)

where \mathbf{v} is the velocity; μ_{EO} and $\mu_{EP,L}$ are the linear EO and EP mobilities, respectively; ε_m and η denote the permittivity and viscosity of the suspending buffer medium, respectively; and ζ_W and ζ_P denote the zeta potentials of the channel wall and particle, respectively. The nonlinear EK phenomena considered here are dielectrophoresis (DEP) and nonlinear EP (EPNL). The expression of the DEP velocity of a spherical particle is as follows:

$$\mathbf{v}_{DEP} = \mu_{DEP} \nabla E_{rms}^2 = \frac{r_p^2 \varepsilon_m}{3\eta} Re[f_{CM}] \nabla E_{rms}^2$$
 (3)

where r_p is the particle radius; $Re[f_{CM}]$ is the real part of the Clausius–Mossotti factor, accounting for polarization effects; and E_{rms} is the root mean square value of E. Regarding the velocity expressions for EP_{NL} , the dimensionless applied field strength coefficient (β) and Peclet (Pe) and Dukhin (Du) numbers are required to identify the appropriate electric field dependence. There are only two limiting cases described using mathematical expressions for $\mathbf{v}_{EP,NL}$, which are small Pe $(Pe \ll 1)$ and high Pe $(Pe \gg 1)$. There are no well-established analytical expressions for the intermediate cases. The velocity expressions for these two limiting cases are given below [42,45,46]:

$$\mathbf{v}_{EP,NL}^{(3)} = \mu_{EP,NL}^{(3)} E^3 \hat{\mathbf{a}}_E$$
 for $\beta \sim 1$, arbitrary Du , and $Pe \ll 1$ (moderate field regime) (4)

$$\mathbf{v}_{EP,NL}^{(3/2)} = \mu_{EP,NL}^{(3/2)} \hat{\mathbf{a}}_E$$
 for $\beta > 1$, $Du << 1$, and $Pe >> 1$ (strong field regime) (5)

where $\mu_{EP,NL}^{(n)}$ denotes the mobility of EP_{NL}, which depends on E [41], and n denotes the dependence of $\mathbf{v}_{EP,NL}$ on \mathbf{E} as dictated by the operating conditions (see Table S1 in supplementary material). Considering these four distinct EK phenomena, the overall particle/cell velocity (\mathbf{v}_P) in an iEK device as represented in Figure 1, is:

$$\mathbf{v}_{P} = \mathbf{v}_{EO} + \mathbf{v}_{EP,L} + \mathbf{v}_{DEP} + \mathbf{v}_{EP,NL}^{(n)} = \mu_{EO} \mathbf{E} + \mu_{EP,L} \mathbf{E} + \mu_{DEP} \nabla E^{2} + \mu_{EP,NL}^{(n)} E^{n} \hat{\mathbf{a}}_{E}$$
(6)

The quality of each of the separations was quantified in terms of the separation resolution (R_s) , calculated as follows from the electropherograms:

$$R_{s} = \frac{2(t_{R2,e} - t_{R1,e})}{W_{1} + W_{2}} \tag{7}$$

where W and $t_{R,e}$ denote the width of the peak at the base and the experimental retention time of each eluting species, respectively (Figure S1).

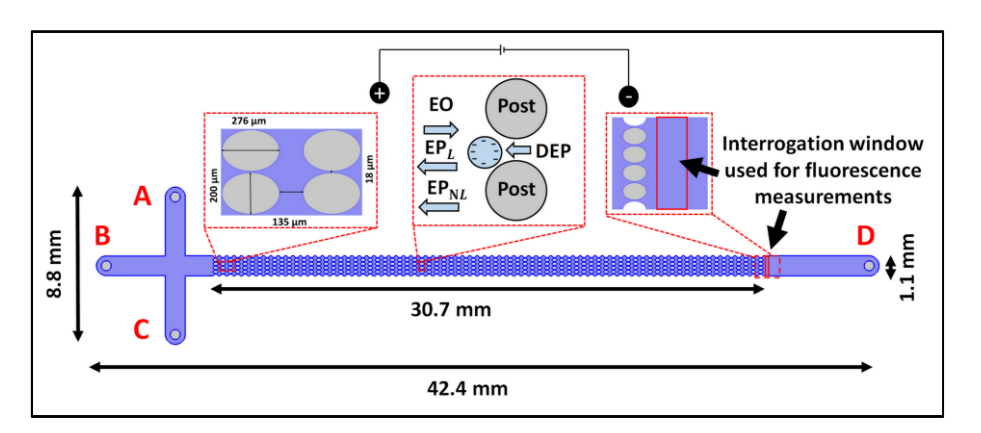


Figure 1. Schematic illustration of the iEK microchannel with four reservoirs labeled A–D, depicting the channel dimensions and the location of the interrogation window used for measuring fluorescence. The first figure inset shows the post dimensions. The second figure inset illustrates the four EK forces (EO, EP_L, EP_{NL}, and DEP) acting on the cells, which possess a negative surface charge and feature a smaller complex permittivity than the suspending solution. The third figure inset indicates the interrogation widow used for fluorescence measurements of the cells eluting from the post array and the walls of the microchannel.

3. Materials and Methods

3.1. Fabrication of Microdevices

A cross-T iEK microchannel (Figure 1) was fabricated from polydimethylsiloxane (PDMS) using traditional soft lithography techniques [29]. After curing and gently detaching the PDMS casts of the microchannel, holes for inlet and outlet reservoirs were punched. The device fabrication process was completed by sealing the PDMS microchannel with a PDMS-coated glass wafer using corona treatment. The detailed dimensions of the microchannel, which was 30 μ m deep, are provided in Figure 1.

3.2. Suspending Medium and Cell Samples

The suspending medium was a 0.2 mM solution of K₂HPO₄ with 0.05% (v/v) Tween-20. The pH and conductivity of the medium were adjusted to 7.1 ± 0.4 and 41.3 ± 5 µS/cm, respectively, by adding 0.1 N KOH solution. These conditions resulted in ζ_W and μ_{EO} of -60.1 ± 3.7 mV and $4.7 \pm 0.3 \times 10^{-8}$ m² V⁻¹ s⁻¹, respectively, which were measured experimentally using current monitoring experiments [47]. The two types of cells studied in this work were E.~coli (ATCC 11775) and S.~cerevisiae (ATCC 9763), whose properties are listed in Table 1. Standard procedures were used to culture and stain the cells using fluorescent SYTO dyes—Syto 11 (green) nucleic acid stain and Syto 85 (orange) nucleic acid stain (Thermo Fisher Scientific, Carlsbad, CA, USA) [7]. The values of ζ_P , $\mu_{EP,L}$, and $\mu_{EP,NL}^{(3)}$ for both types of cells, possessing a negative surface charge, were independently measured using PTV experiments using a channel with a constant cross-section [48]. A binary mixture of these cells was injected into the iEK microchannel (Figure 1) using EK injection [49].

Table 1. Characteristics of the cells used in this study.

Cell ID	Size (µm)	ζ _P (mV)	$\mu_{EP,L} \times 10^{-8}$ (m ² V ⁻¹ s ⁻¹)	$\mu_{EP,NL}^{(3)} \times 10^{-18}$ (m ⁴ V ⁻³ s ⁻¹)
E. coli (ATCC 11775)	$3.2 \pm 0.3 $ long $1.1 \pm 0.2 $ wide	-25.3 ± 2.1 ²	-1.97 ± 0.1 ²	-2.1 ± 0.1 1,2
S. cerevisiae (ATCC 9763)	7.0 ± 0.7 diameter	-29.1 ± 3.7 ²	-2.26 ± 0.3 ²	-7.6 ± 1.5 ^{1,2}

¹ Average approximation obtained through analytical curve fitting of cubic dependence of EP_{NL} velocity on **E**. ² Characteristics such as ζ_P , $\mu_{EP,L}$, and $\mu_{EP,NL}^{(3)}$ mobilities depend on the suspending medium and are specific to these cell–fluid systems.

3.3. Equipment and Software

A high-voltage power supply (Model HVS6000D, LabSmith, Livermore, CA, USA) controlled using LabSmith Sequencer software version 1.167 was used to apply voltage to the microchannels through platinum wire electrodes (0.584 mm diameter and 1.5 cm length) labeled A–D (Figure 1). Experiments were recorded as videos using a Zeiss Axiovert 40 CFL (Carl Zeiss Microscopy, Thornwood, NY, USA) inverted microscope.

3.4. Experimental Procedure

Before experimentation, the microchannel was filled with the suspending medium to ensure stable EO flow. The cell mixture sample (~5 μL), comprising E. coli (5 \pm 0.8 \times 108 cells/mL) and S. cerevisiae (1 \pm 0.6 \times 108 cells/mL), was introduced into inlet reservoir A of the microchannel (Figure 1), after which the platinum electrodes were placed at each reservoir. A standard EK injection process [49], performed via sequential application of the voltages listed in Table 2, was used to inject the sample mixture to the post array region of the microchannel. The last step of the separation was determined by the elution of the cells from the channel. The fluorescence signal of each eluting cell species was captured at the end of the post array, as indicated in the interrogation window (Figure 1). Each of the two separations was repeated thrice to ensure reproducibility (Table S3).

Separation	Description	Step	Run Time	Applied Voltage (V)	
ID	Description		(s)	A	В	C	D
		Loading (DC)	10	500	300	0	500
1	Separation using	Gating (DC)	5	1000	1000	1000	0
	DC potential	Injection (DC)	5	0	1000	0	0
		Separation (DC)	450	200	656	200	0
		Loading (DC)	10	500	300	0	500
		Gating (DC)	5	1000	1000	1000	0
	Separation using	Injection (DC)	5	0	1000	0	0
2	DC-biased AC po-			500 (DC)			
	tential	Separation (DC	450	200	+ 600	200	0
		bias + AC)			(V_p) @		
					$0.4~\mathrm{Hz}$		

Table 2. Voltage conditions used for EK injection and separation of the cells.

3.5 Mathematical Modeling

Numerical models were built using COMSOL Multiphysics for predicting retention time ($t_{R,p}$), which was compared to the experimental retention time ($t_{R,e}$) of each cell type. The cell characteristics, assessed a priori [48], were utilized for predicting $t_{R,p}$ in the microchannel for each cell type with the appropriate stimulation voltage. Details on the mathematical model are included in the Supplementary Material (Figures S2–S5, Table S2).

4. Results and Discussion

4.1. Separation of Cells by Applying DC Signal

To design the DC signal, the RMS value for the DC-biased AC voltage (used for Separation ID 2) was employed, as listed in Table 2. The experimental results from the separation of this binary cell mixture are shown in Figure 2. The cells appeared to be mixed with each other as they migrated across the post array (Figure 2A), indicating that no appreciable separation was taking place. This can be confirmed by the electropherogram in

Figure 2B, featuring an overlap of the eluting peaks, with a poor separation resolution of $R_s = 0.55$, indicating that the separation was incomplete ($R_s < 1.5$). It can be noted from the electropherogram that although there was overlap in the elution of the cells, the E. coli cells reached the interrogation window slightly before the S. cerevisiae cells. This can be explained by the ζ_P and $\mu_{EP,L}$ values of the cells (Table 1). Good reproducibility, indicated by <10% deviation between repetitions, was obtained (Table S3). The deviation between model and experimental results, in terms of retention time, was below 19% (Table 3), illustrating that the model is a good tool for predicting the performance of this separation and can be used to design new separations. The COMSOL model was also used to study the effect of each individual EK phenomenon on the overall cell velocity across a cutline (Figure S3) between post constrictions, where the minimal effect of EPNL on both cell species indicated that the separation was mainly in the linear regime (Figure S5A,B). In summary, the incomplete separation obtained by applying a DC voltage equivalent to the RMS value of the DC-biased AC voltage highlighted that for the cell mixture under consideration (Table 1), application of DC voltage alone was not sufficient to discriminate and separate the cells.

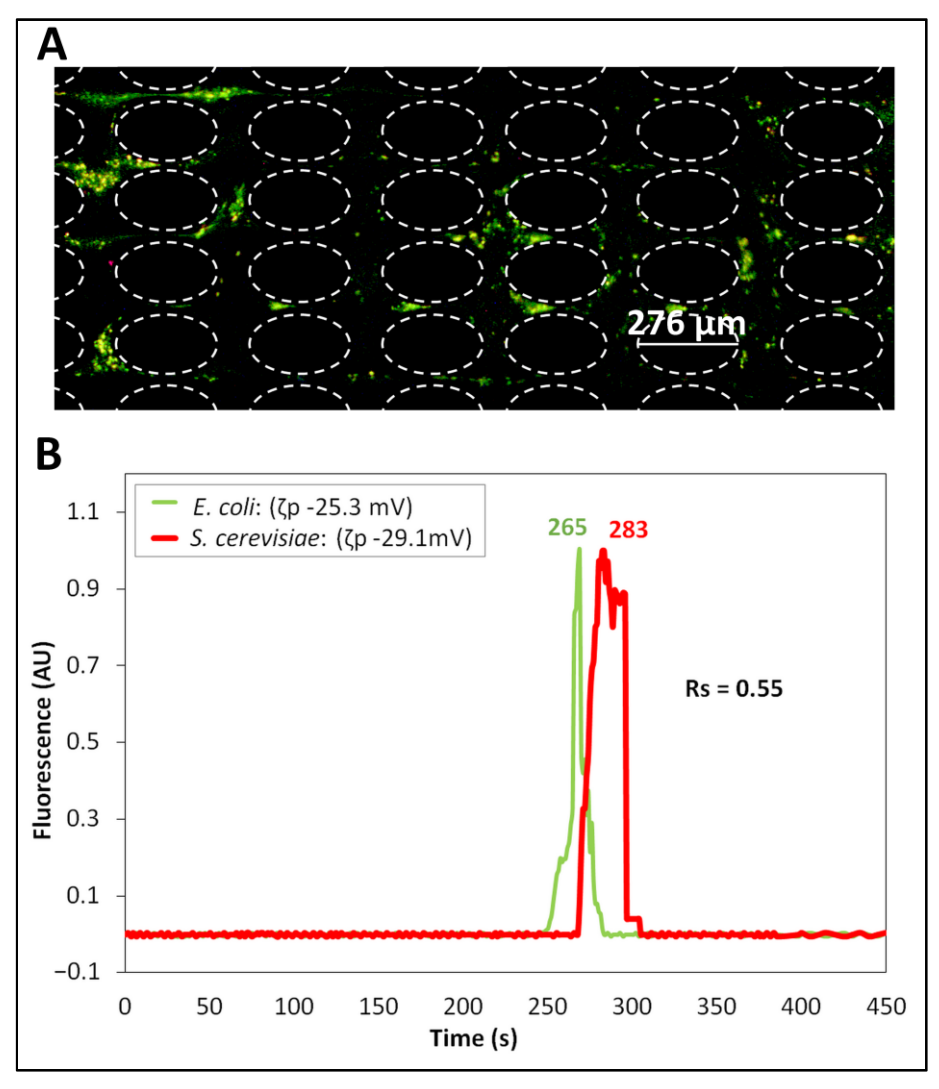


Figure 2. Separation (ID 1) of the cells performed by applying a DC voltage. (**A**) Image of the post array, where cell species are migrating while mixed with each other, i.e., the *E. coli* cells (labeled green) and the *S. cerevisiae* cells (labeled red) are interspersed. (**B**) Electropherogram of the separa-

tion built from the fluorescence signal of the cells recorded at the interrogation window. This separation was performed by applying a DC voltage with a 656 V magnitude, which was equivalent to the RMS value of the DC-biased AC voltage used for Separation ID 2.

Table 3. Assessment of the separations in terms of R_s , comparison of $t_{R,p}$ and $t_{R,e}$, and reproducibility between separation experiments.

Separation ID	Cell ID	R_s		Average of Experimental $t_{R,e}$ (s)	Deviation between $t_{R,p}$ and $t_{R,e}$ (%)	Experimental Deviation between Repetitions (%)
1	E. coli	0.55	197.0	239.7	17.8	7.8
	S. cerevisiae		224.2	274.3	18.3	6.6
2	E. coli	1.51	228.6	241.7	5.4	2.5
	S. cerevisiae		261.3	295.7	11.6	2.6

4.2. Separation of Cells by Applying DC-Biased Low-Frequency AC Signal

The second separation was carried out by applying a DC-biased low-frequency AC electric voltage, which was carefully selected from COMSOL simulations to have a difference between the predicted retention times of the cells of at least 30 s. Our previous work established that a difference of at least 30 s ($\Delta t_{R,p} > 30$ s) is required for a separation to be successful [43]. The identified voltage was a 500 V DC-biased 600 V peak amplitude at 0.4 Hz frequency. This AC voltage was the one "mimicked" by the DC voltage used in Separation ID 1. Since successful separation of microparticles and cells has been previously reported at 0.4 Hz [29,43], this was chosen as the frequency for these separation experiments. The experimental results of this separation are shown in Figure 3. The image in Figure 3A shows the formation of "zones" of E. coli and S. cerevisiae cells as they migrated across the insulating post array. The green-labeled E. coli cells were migrating ahead of the red-labeled *S. cerevisiae* cells. This result was as expected from the ζ_P and $\mu_{EP,L}$ values of the cells (Table 1), since E. coli cells have lower magnitudes of ζ_P and $\mu_{EP,L}$, allowing these cells to migrate faster towards the outlet and elute first. The electropherogram of this separation is shown in Figure 3B with a separation resolution of $R_s = 1.51$, indicating a complete separation with well-resolved peaks. It is important to acknowledge the non-Gaussian shape of the peaks, which is the result of the back-and-forth movement of the cells due to the AC signal application. Good reproducibility of < 10% was obtained between experimental repetitions for each cell species (Table S3). As conducted with Separation ID 1, the COMSOL model was used to study the effects of the four distinct EK phenomena on the overall cell velocity (Figure S5C,D). For S. cerevisiae cells, there was a moderate effect of EPNL on the overall cell velocity, which was beneficial for the separation. The deviation between model and experimental results, in terms of retention time, was below 12% (Table 3), indicating good agreement and reiterating the applicability of the model for designing new separation processes. Potential causes of the deviations between modeling and experimental results are EK injection bias during the sample injection process, local electric field distortions caused by the particles themselves, and particle-particle interactions, since none of those are accounted for in the model [49].

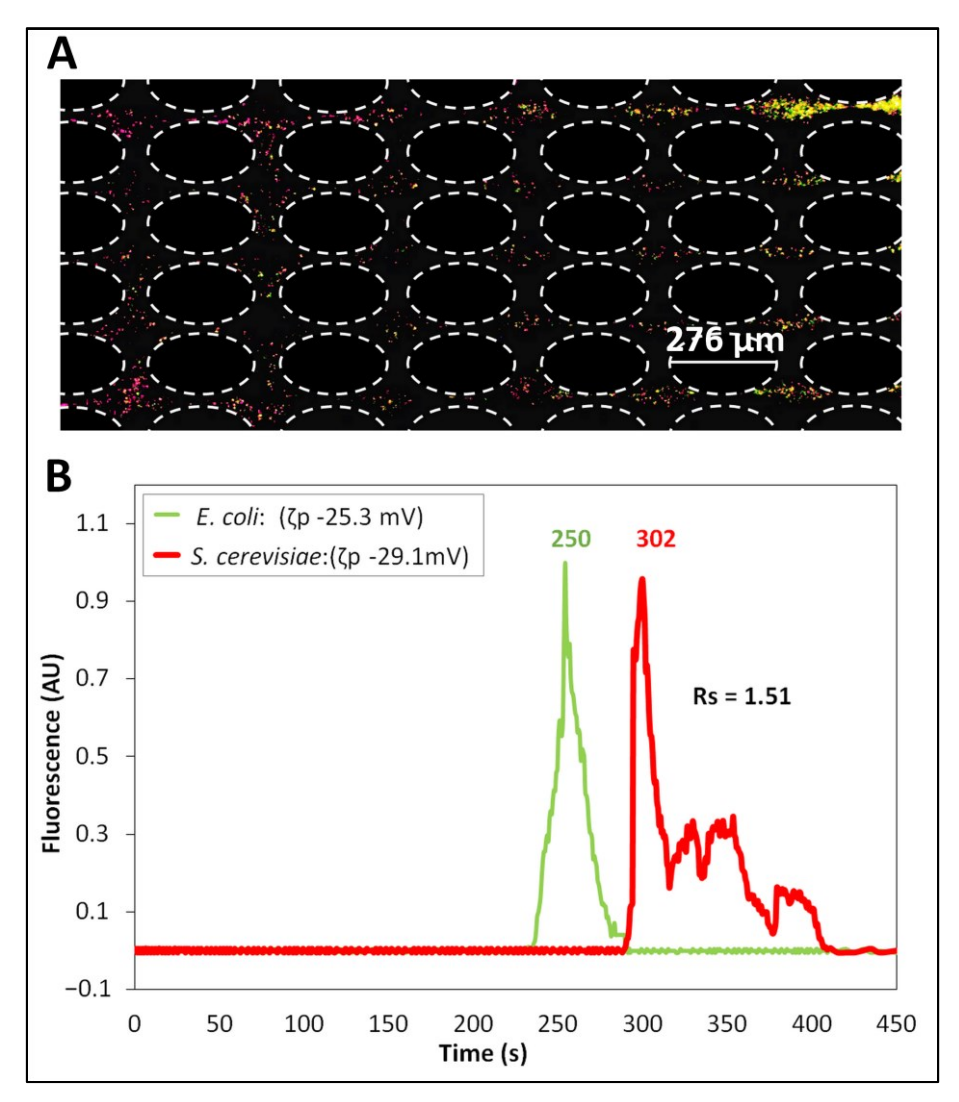


Figure 3. Separation (ID 2) of the cells performed by applying a DC-biased AC voltage. (**A**) Image of the post array, where the cells begin to form "zones" of cells, illustrating that the *E. coli* cells (labeled green) are moving ahead of the *S. cerevisiae* cells (labeled red). (**B**) Electropherogram of the separation obtained by analyzing the fluorescence signal of the cells, recorded at the interrogation window. This separation was performed by applying a DC-biased AC voltage having 500 V DC bias and 600 V peak amplitude at 0.4 Hz.

4.3. Comparison of the Separation Effectiveness Obtained with the DC Voltages and with the DC-Biased Low-Frequency AC Voltages

The separation of cells is mainly governed by the differences in the overall cell velocity, as expressed in Equation (6), which depends on the individual velocity components of the four EK phenomena, as shown in Equations (1)–(5). The magnitudes of all EK phenomena depend on the electric field and the position of the cells in the iEK channel. For both the separations (Separation IDs 1–2), the nonuniform electric field across the iEK channel, caused by the presence of insulating posts, exerted a combination of linear and nonlinear EK effects on the cells, which affected their overall velocities (Figure S5). For Separation ID 1, employing a DC potential, whose only relevant characteristic was its magnitude, the electric field distribution did not vary with time; therefore, its maximum magnitude was not time-dependent either. In contrast, for Separation ID 2, employing a DC-biased AC potential, which had a temporal component, the electric field distribution was time-dependent, and the maximum electric field magnitude was reached at the time of peak amplitude application. The prediction of overall cell velocity for both *E. coli* and *S. cerevisiae* cells across a cutline between two posts' constrictions (cutline shown in Figure

S3), at the maximum magnitude of the electric field, for both separations (Separation IDs 1–2) is shown in Figure 4. The difference between the two distinct cell velocities for Separation ID 1 (Figure 4A), employing a DC voltage, was much smaller than that obtained with Separation ID 2 (Figure 4B), employing a DC-biased AC potential. This larger difference between the two distinct overall cell velocities obtained with the DC-biased AC potential at the maximum electric field magnitude, at the time of peak amplitude application, increased the discrimination capability between the two cell species. Therefore, the application of the DC-biased AC potential resulted in a complete separation ($R_s = 1.51$), compared to the incomplete separation ($R_s = 0.55$) obtained by applying the DC potential.

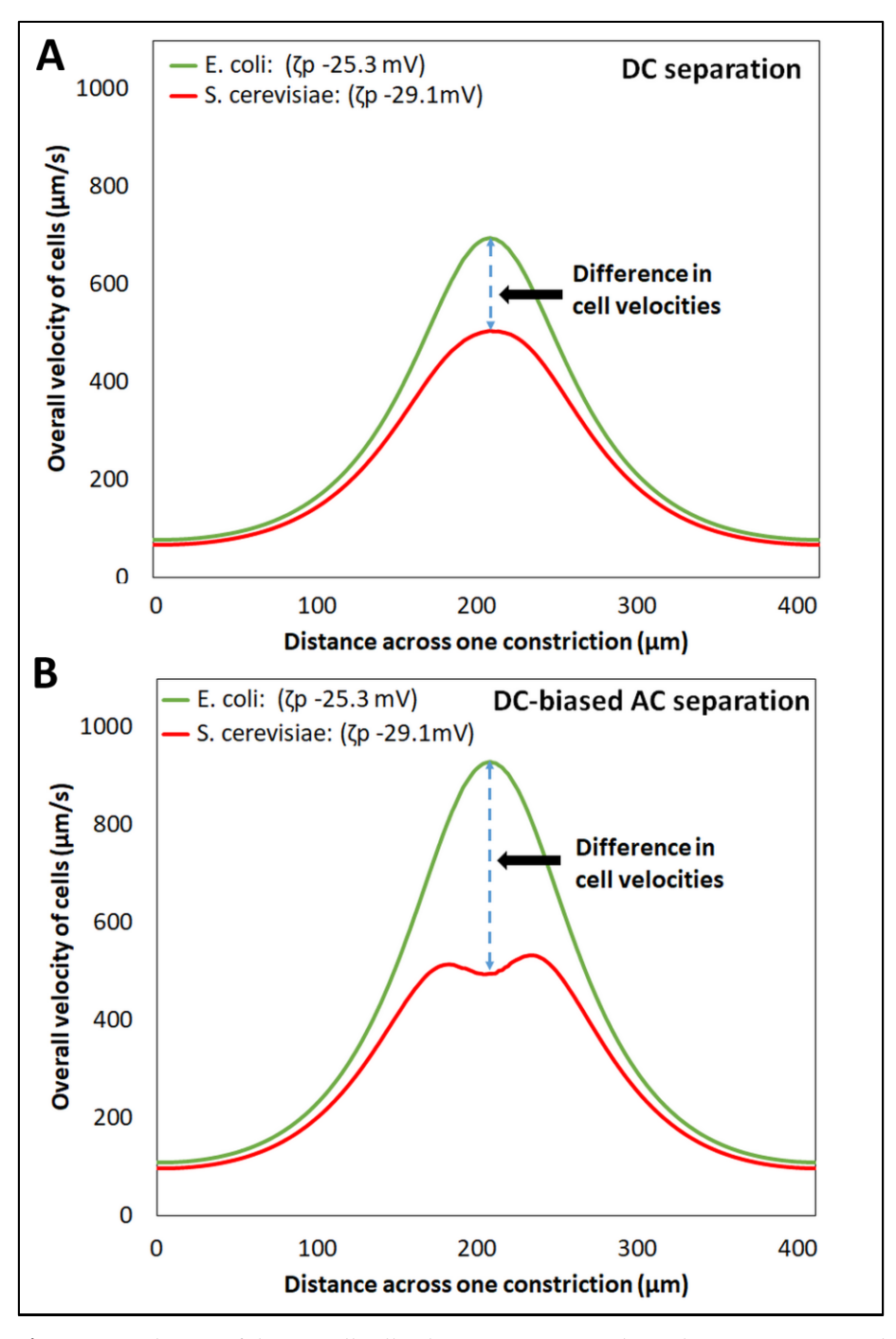


Figure 4. Prediction of the overall cell velocities across a cutline (shown in Figure S3) between two posts' constrictions, with the two types of separation—(**A**) Separation ID 1, employing a DC potential at 656 V, and (**B**) Separation ID 2, employing a DC-biased AC voltage having 500 V DC bias and 600 V peak amplitude at 0.4 Hz, respectively.

5. Conclusions

Presented here is the separation of a binary mixture of cells (E. coli and S. cerevisiae) in an iEK microchannel employing two distinct electric stimulations: a DC voltage and a low-frequency DC-biased AC voltage. The magnitude of the DC voltage was designed to be equivalent in magnitude to the RMS of the DC-biased AC voltage. Mathematical modeling with COMSOL was used to guide experimentation (selection of appropriate electric voltages to apply) and to gain understanding of the effect of the four distinct different EK phenomena influencing cell migration behavior. The iEK separation employing the DC voltage had poor performance, with a separation resolution of $R_s = 0.55$, while the separation with the DC-biased AC voltage resulted in a complete separation, with R_s = 1.51. The two distinct separations had good experimental reproducibility, with deviations below 10% between experimental repetitions. Good agreement was also obtained between modeling and experimental results, with deviations below 19% for all cases. This is the first study to compare the separation performance of a binary mixture of cells in an iEK device by applying two types of potential: a DC potential and a DC-biased AC potential. The results from this work highlight the importance of the type of electric stimulation being used for the same separation in the same iEK device geometry. The main finding from this study is that the cell mixture under consideration remains mixed and does not separate when using a DC voltage but it is effectively separated using a DC-biased AC voltage.

This follow-up study to our previous study on fine-tuning low-frequency AC voltages to improve the separation resolution of mixtures of microparticles demonstrates the discriminatory capability of AC-iEK systems to enable cell separations, which cannot be achieved with their DC-iEK counterpart. The ability of AC voltages to effectively discriminate cells opens up the potential for future research to separate microscopic entities of interest using an iEK system stimulated with AC potentials at different low frequencies and investigate the effect of frequency on cell separations. Future contributions to this field will assess the application of AC-iEK systems to separate cells or particles with more similar characteristics, evaluate the influence of the microchannel wall on the experimental results of separation, and extend the applications of these systems to complex mixtures containing three or more distinct target analytes.

Supplementary Materials: The following supporting information can be downloaded at www.mdpi.com/xxx/s1, Table S1: Values of the parameters used to analyze the moderate field regime, cubic dependence (E³); Table S2: COMSOL model information; Table S3: Experimental repetitions of separations; Figure S1: Illustration of peaks in an electropherogram; Figure S2: Depiction of domains and boundaries used in computational model; Figure S3: Representation of the cutline constructed in COMSOL Multiphysics to determine predicted retention time for the cells to migrate across the insulating post array; Figure S4: Curve-fitting results using a Fourier series expansion of the E-field profile; Figure S5: Prediction of the overall and individual cell velocities of the four EK phenomena across the cutline, with the two types of separation (Separation IDs 1–2); Video S1: Separation by applying DC potential; Video S2: Separation achieved by applying DC-biased AC potential

Author Contributions: Conceptualization, V.H.P.-G. and B.H.L.-E.; methodology, V.H.P.-G. and B.H.L.-E.; experimental data curation, N.N.N.A. and C.A.M.-E.; COMSOL simulations, N.N.N.A. and C.A.M.-E.; writing—review and editing, N.N.N.A., C.A.M.-E., V.H.P.-G., and B.H.L.-E.; supervision, V.H.P.-G. and B.H.L.-E.; project administration, V.H.P.-G. and B.H.L.-E.; funding acquisition, V.H.P.-G. and B.H.L.-E. All authors have read and agreed to the published version of the manuscript.

Funding: This study is based upon work supported by the National Science Foundation under Award No. 2127592. The authors also acknowledge support from the Kate Gleason College of Engineering, the Nano-Sensors & Devices Research Group (0020209I06) and the Federico Baur Endowed Chair in Nanotechnology (0020240I03) and the Mechatronics and Electrical Engineering Department at Tecnologico de Monterrey.

Data Availability Statement: Data are contained within the article and Supplementary Materials.

Acknowledgments: The authors also acknowledge the valuable contribution provided by Alaleh Vaghef-Koodehi in helping with training and experiments.

Conflicts of Interest: The authors declare no conflict of interest. The funders had no role in the design of the study; in the collection, analyses, or interpretation of data; in the writing of the manuscript; or in the decision to publish the results.

References

- Rajapaksha, P.; Elbourne, A.; Gangadoo, S.; Brown, R.; Cozzolino, D.; Chapman, J. A Review of Methods for the Detection of Pathogenic Microorganisms. *Analyst* 2019, 144, 396–411. https://doi.org/10.1039/C8AN01488D.
- 2. Dorsey, J.G. Introduction to Modern Liquid Chromatography, 3rd Ed. J. Am. Chem. Soc. 2010, 132, 9220–9220. https://doi.org/10.1021/ja104156b.
- Klepárník, K. Recent Advances in Combination of Capillary Electrophoresis with Mass Spectrometry: Methodology and Theory. Electrophoresis 2015, 36, 159–178.
- 4. Ding, J.; Woolley, C.; Hayes, M.A. Biofluid Pretreatment Using Gradient Insulator-Based Dielectrophoresis: Separating Cells from Biomarkers. *Anal. Bioanal. Chem.* **2017**, 409, 6405–6414. https://doi.org/10.1007/s00216-017-0582-5.
- 5. Xuan, X. Recent Advances in Direct Current Electrokinetic Manipulation of Particles for Microfluidic Applications. *Electrophoresis* **2019**, *40*, 2484–2513. https://doi.org/10.1002/elps.201900048.
- 6. Ding, J.; Lawrence, R.M.; Jones, P.V.; Hogue, B.G.; Hayes, M.A. Concentration of Sindbis Virus with Optimized Gradient Insulator-Based Dielectrophoresis. *Analyst* 2016, 141, 1997–2008. https://doi.org/10.1039/C5AN02430G.
- 7. Vaghef-Koodehi, A.; Ernst, O.D.; Lapizco-Encinas, B.H. Separation of Cells and Microparticles in Insulator-Based Electrokinetic Systems. *Anal. Chem.* **2023**, *95*, 1409–1418. https://doi.org/10.1021/acs.analchem.2c04366.
- 8. Desai, M.J.; Armstrong, D.W. Separation, Identification, and Characterization of Microorganisms by Capillary Electrophoresis. *Microbiol. Mol. Biol. Rev.* **2003**, *67*, 38–51. https://doi.org/10.1128/mmbr.67.1.38-51.2003.
- 9. Girod, M.; Armstrong, D.W. Monitoring the Migration Behavior of Living Microorganisms in Capillary Electrophoresis Using Laser-Induced Fluorescence Detection with a Charge-Coupled Device Imaging System. *Electrophoresis* **2002**, 23, 2048–2056.
- Rodriguez, M.A.; Armstrong, D.W. Separation and Analysis of Colloidal/Nano-Particles Including Microorganisms by Capillary Electrophoresis: A Fundamental Review. J. Chromatogr. B 2004, 800, 7–25.
- 11. Schneiderheinze, J.M.; Armstrong, D.W.; Schulte, G.; Westenberg, D.J. High Efficiency Separation of Microbial Aggregates Using Capillary Electrophoresis. *FEMS Microbiol. Lett.* **2000**, *189*, 39–44.
- 12. Armstrong, D.W.; Schulte, G.; Schneiderheinze, J.M.; Westenberg, D.J. Separating Microbes in the Manner of Molecules. 1. Capillary Electrokinetic Approaches. *Anal. Chem.* **1999**, *71*, 5465–5469. https://doi.org/10.1021/ac990779z.
- 13. Horká, M.; Karásek, P.; Růžička, F.; Dvořáčková, M.; Sittová, M.; Roth, M. Separation of Methicillin-Resistant from Methicillin-Susceptible Staphylococcus Aureus by Electrophoretic Methods in Fused Silica Capillaries Etched with Supercritical Water. *Anal. Chem.* **2014**, *86*, 9701–9708. https://doi.org/10.1021/ac502254f.
- 14. Horká, M.; Šalplachta, J.; Karásek, P.; Růžička, F.; Štveráková, D.; Pantůček, R.; Roth, M. Rapid Isolation, Propagation, and Online Analysis of a Small Number of Therapeutic Staphylococcal Bacteriophages from a Complex Matrix. *ACS Infect. Dis.* **2020**, *6*, 2745–2755. https://doi.org/10.1021/acsinfecdis.0c00358.
- 15. Horká, M.; Šalplachta, J.; Karásek, P.; Růžička, F.; Roth, M. Online Concentration of Bacteria from Tens of Microliter Sample Volumes in Roughened Fused Silica Capillary with Subsequent Analysis by Capillary Electrophoresis and Matrix-Assisted Laser Desorption/Ionization Time-of-Flight Mass Spectrometry. *ACS Infect. Dis.* **2020**, *6*, 355–365. https://doi.org/10.1021/acsinfecdis.9b00200.
- 16. Šalplachta, J.; Horká, M.; Růžička, F.; Šlais, K. Identification of Bacterial Uropathogens by Preparative Isoelectric Focusing and Matrix-Assisted Laser Desorption/Ionization Time-of-Flight Mass Spectrometry. *J. Chromatogr. A* **2018**, *1532*, 232–237. https://doi.org/10.1016/j.chroma.2017.11.072.
- 17. Horká, M.; Šlais, K.; Šalplachta, J.; Růžička, F. Preparative Isoelectric Focusing of Microorganisms in Cellulose-Based Separation Medium and Subsequent Analysis by CIEF and MALDI-TOF MS. *Anal. Chim. Acta* **2017**, 990, 185–193. https://doi.org/10.1016/j.aca.2017.08.046.
- 18. Dziubakiewicz, E.; Buszewski, B. Applications of Electromigration Techniques: Electromigration Techniques in Detection of Microorganisms. In *Electromigration Techniques: Theory and Practice*; Buszewski, B., Dziubakiewicz, E., Szumski, M., Eds.; Springer: Berlin/Heidelberg, Germany, 2013; pp. 287–298, ISBN 978-3-642-35043-6.
- 19. Buszewski, B.; Maślak, E.; Złoch, M.; Railean-Plugaru, V.; Kłodzińska, E.; Pomastowski, P. A New Approach to Identifying Pathogens, with Particular Regard to Viruses, Based on Capillary Electrophoresis and Other Analytical Techniques. *TrAC-Trends Anal. Chem.* **2021**, 139, 116250. https://doi.org/10.1016/J.TRAC.2021.116250.
- Buszewski, B.; Król, A.; Pomastowski, P.; Railean-Plugaru, V.; Szultka-Młyńska, M. Electrophoretic Determination of Lactococcus Lactis Modified by Zinc Ions. Chromatographia 2019, 82, 347–355. https://doi.org/10.1007/s10337-018-3665-3.
- 21. Pomastowski, P.; Railean-Plugaru, V.; Buszewski, B. Microbial Analysis of Escherichia Coli Atcc, Lactobacteria and Saccharomyces Cerevisiae Using Capillary Electrophoresis Approach. In *Methods in Molecular Biology*; Humana Press Inc.: Totowa, NJ, USA, 2016; Volume 1483, pp. 393–406.

- 22. Buszewski, B.; Szumski, M.; Kłodzińska, E.; Dahm, H. Separation of Bacteria by Capillary Electrophoresis. *J. Sep. Sci.* 2003, 26, 1045–1049. https://doi.org/10.1002/jssc.200301442.
- 23. Liu, Y.; Hayes, M.A. Differential Biophysical Behaviors of Closely Related Strains of Salmonella. *Front. Microbiol.* **2020**, *11*, 302. https://doi.org/10.3389/fmicb.2020.00302.
- 24. Crowther, C.V.; Hilton, S.H.; Kemp, L.K.; Hayes, M.A. Isolation and Identification of *Listeria Monocytogenes* Utilizing DC Insulator-Based Dielectrophoresis. *Anal. Chim. Acta* 2019, 1068, 41–51. https://doi.org/10.1016/j.aca.2019.03.019.
- 25. Hilton, S.H.; Crowther, C.V.; McLaren, A.; Smithers, J.P.; Hayes, M.A. Biophysical Differentiation of Susceptibility and Chemical Differences in: Staphylococcus Aureus. *Analyst* **2020**, *145*, 2904–2914. https://doi.org/10.1039/c9an01449g.
- Ros, A.; Eichhorn, R.; Regtmeier, J.; Duong, T.T.; Reimann, P.; Anselmetti, D. Absolute Negative Particle Mobility. Nature 2005, 436, 928. https://doi.org/10.1038/436791a.
- 27. Luo, J.; Muratore, K.A.; Arriaga, E.A.; Ros, A. Deterministic Absolute Negative Mobility for Micro- and Submicrometer Particles Induced in a Microfluidic Device. *Anal. Chem.* **2016**, *88*, 5920–5927. https://doi.org/10.1021/acs.analchem.6b00837.
- 28. Kim, D.; Luo, J.; Arriaga, E.A.; Ros, A. Deterministic Ratchet for Sub-Micrometer (Bio)Particle Separation. *Anal. Chem.* **2018**, 90, 4370–4379. https://doi.org/10.1021/acs.analchem.7b03774.
- 29. Saucedo-Espinosa, M.A.; Lalonde, A.; Gencoglu, A.; Romero-Creel, M.F.; Dolas, J.R.; Lapizco-Encinas, B.H. Dielectrophoretic Manipulation of Particle Mixtures Employing Asymmetric Insulating Posts. *Electrophoresis* **2016**, 37, 282–290. https://doi.org/10.1002/elps.201500195.
- 30. Church, C.; Zhu, J.J.; Wang, G.Y.; Tzeng, T.R.J.; Xuan, X.C. Electrokinetic Focusing and Filtration of Cells in a Serpentine Microchannel. *Biomicrofluidics* **2009**, *3*, 44109–44110. https://doi.org/10.1063/1.3267098.
- 31. Malekanfard, A.; Beladi-Behbahani, S.; Tzeng, T.-R.; Zhao, H.; Xuan, X. AC Insulator-Based Dielectrophoretic Focusing of Particles and Cells in an "Infinite" Microchannel. *Anal. Chem.* **2021**, *93*, 5947–5953. https://doi.org/10.1021/acs.analchem.1c00697.
- 32. Calero, V.; Fernández-Mateo, R.; Morgan, H.; García-Sánchez, P.; Ramos, A. Low-Frequency Electrokinetics in a Periodic Pillar Array for Particle Separation. *J. Chromatogr. A* 2023, 1706, 464240. https://doi.org/10.1016/j.chroma.2023.464240.
- 33. Calero, V.; Garcia-Sanchez, P.; Honrado, C.; Ramos, A.; Morgan, H. AC Electrokinetic Biased Deterministic Lateral Displacement for Tunable Particle Separation. *Lab. Chip* **2019**, *19*, 1386–1396. https://doi.org/10.1039/c8lc01416g.
- 34. Perez-Gonzalez, V.H. Particle Trapping in Electrically Driven Insulator-Based Microfluidics: Dielectrophoresis and Induced-Charge Electrokinetics. *Electrophoresis* **2021**, 42, 2445–2464. https://doi.org/10.1002/elps.202100123.
- 35. Dukhin, S.S. Electrokinetic Phenomena of the Second Kind and Their Applications. *Adv. Colloid. Interface Sci.* **1991**, *35*, 173–196. https://doi.org/10.1016/0001-8686(91)80022-C.
- 36. Mishchuk, N.A.; Barinova, N.O. Theoretical and Experimental Study of Nonlinear Electrophoresis. *Colloid. J.* **2011**, 73, 88–96. https://doi.org/10.1134/S1061933X11010133.
- 37. Hill, N.; Lapizco-Encinas, B.H. On the Use of Correction Factors for the Mathematical Modeling of Insulator Based Dielectrophoretic Devices. *Electrophoresis* **2019**, *40*, 2541–2552. https://doi.org/10.1002/elps.201900177.
- 38. Bentor, J.; Dort, H.; Chitrao, R.A.; Zhang, Y.; Xuan, X. Nonlinear Electrophoresis of Dielectric Particles in Newtonian Fluids. *Electrophoresis* **2023**, 44, 938–946. https://doi.org/10.1002/elps.202200213.
- 39. Rouhi Youssefi, M.; Diez, F.J. Ultrafast Electrokinetics. Electrophoresis 2016, 37, 692–698. https://doi.org/10.1002/elps.201500392.
- 40. Tottori, S.; Misiunas, K.; Keyser, U.F.; Bonthuis, D.J. Nonlinear Electrophoresis of Highly Charged Nonpolarizable Particles. *Phys. Rev. Lett.* **2019**, 123, 14502. https://doi.org/10.1103/PhysRevLett.123.014502.
- 41. Khair, A.S. Nonlinear Electrophoresis of Colloidal Particles. Curr. Opin. Colloid. Interface Sci. 2022, 59, 101587.
- 42. Cobos, R.; Khair, A.S. Nonlinear Electrophoretic Velocity of a Spherical Colloidal Particle. *J. Fluid. Mech.* **2023**, 968, A14. https://doi.org/10.1017/jfm.2023.537.
- 43. Nihaar, N.; Ahamed, N.; Mendiola-Escobedo, C.A.; Ernst, O.D.; Perez-Gonzalez, V.H.; Lapizco-Encinas, B.H. Fine-Tuning the Characteristic of the Applied Potential To Improve AC-IEK Separations of Microparticles. *Anal. Chem.* **2023**, *95*, 9914–9923. https://doi.org/10.1021/ACS.ANALCHEM.3C00995.
- 44. Gallo-Villanueva, R.C.; Perez-Gonzalez, V.H.; Cardenas-Benitez, B.; Jind, B.; Martinez-Chapa, S.O.; Lapizco-Encinas, B.H. Joule Heating Effects in Optimized Insulator-Based Dielectrophoretic Devices: An Interplay between Post Geometry and Temperature Rise. *Electrophoresis* **2019**, *40*, 1408–1416. https://doi.org/10.1002/elps.201800490.
- 45. Schnitzer, O.; Zeyde, R.; Yavneh, I.; Yariv, E. Weakly Nonlinear Electrophoresis of a Highly Charged Colloidal Particle. *Phys. Fluids* **2013**, 25, 052004. https://doi.org/10.1063/1.4804672.
- 46. Schnitzer, O.; Yariv, E. Nonlinear Electrophoresis at Arbitrary Field Strengths: Small-Dukhin-Number Analysis. *Phys. Fluids* **2014**, *26*, 122002. https://doi.org/10.1063/1.4902331.
- 47. Saucedo-Espinosa, M.A.; Lapizco-Encinas, B.H. Refinement of Current Monitoring Methodology for Electroosmotic Flow Assessment under Low Ionic Strength Conditions. *Biomicrofluidics* **2016**, *10*, 033104. https://doi.org/10.1063/1.4953183.
- 48. Cardenas-Benitez, B.; Jind, B.; Gallo-Villanueva, R.C.; Martinez-Chapa, S.O.; Lapizco-Encinas, B.H.; Perez-Gonzalez, V.H. Direct Current Electrokinetic Particle Trapping in Insulator-Based Microfluidics: Theory and Experiments. *Anal. Chem.* **2020**, 92, 12871–12879. https://doi.org/10.1021/acs.analchem.0c01303.
- 49. Breadmore, M.C. Electrokinetic and Hydrodynamic Injection: Making the Right Choice for Capillary Electrophoresis. *Bioanalysis* **2009**, *1*, 889–894.

Disclaimer/Publisher's Note: The statements, opinions and data contained in all publications are solely those of the individual author(s) and contributor(s) and not of MDPI and/or the editor(s). MDPI and/or the editor(s) disclaim responsibility for any injury to people or property resulting from any ideas, methods, instructions or products referred to in the content.